Rayleigh-Brillouin spectra in molecular nitrogen

R. P. Sandoval* and R. L. Armstrong
Physics Department, New Mexico State University, Las Cruces, New Mexico 88003
(Received 11 August 1975)

Rayleigh-Brillouin spectra of gaseous N_2 is measured for light scattered at 15° over a pressure range from 1 to 661 Torr. Spectral profiles are analyzed by means of an appropriate kinetic model. A least-χ^2 method determines the optimum values of the theory parameters: total collision frequency and rotational relaxation number. These parameters are compared with values obtained by other methods. Information provided by light-scattering measurements concerning rotational relaxation in dilute systems is discussed.

I. INTRODUCTION

The spectral distribution of light scattered from density fluctuations in dilute gases has been the subject of several investigations.[1-5] High-resolution experimental spectral profiles may now be obtained as a result of developments in laser-light-scattering spectroscopy. It has been shown that these profiles provide detailed information about the molecular-distribution function. Analysis of light-scattering experiments thus appears to offer the basis for a sensitive probe of the dynamical structure of gases.

Fluctuations in the dielectric constant of the gas are responsible for the scattering of light. These fluctuations are generally coupled to fluctuations in density, temperature, and molecular orientation. For dilute gases near room temperature, however, density fluctuations are completely dominant. The spectrum of light scattered at the angle θ provides information about the time dependence of density fluctuations that have a characteristic wavelength $\lambda_f = 2\pi/K$, where $\vec{K} = \vec{k}_0 - \vec{k}_s$ is the vector difference between the wave vectors of the incident and the scattered light, respectively. The magnitude of $K \cong 2k_0 \sin(\theta/2)$, since $k_0 \cong k_s$ in a gas at normal temperatures. The differential scattering cross section, which may be directly compared with experimental spectral profiles, may be shown[6] to have the form:

$$\sigma(\vec{K}, \omega) = \left[\frac{\sin\phi}{4\pi}\left(\frac{\partial \epsilon}{\partial \rho}\right)_T\right]^4 k_0^4 S(\vec{K}, \omega), \tag{1}$$

where ϕ is the angle between the polarization vector of the incident light and the scattered wave vector $\vec{k}_s$, $(\partial\epsilon/\partial\rho)_T$ is the coupling factor, at constant temperature, between the dielectric constant and the density, and $S(\vec{K}, \omega)$ is the double Fourier transform of the classical limit of Van Hove's density correlation function $G(\vec{r}, t)$.[7]

For dilute systems, $G(\vec{r}, t)$ may be obtained from the solution to an appropriate kinetic equation subject to an initial condition. In polyatomic gases, the kinetic equation proposed by Wang Chang and Uhlenpeck[8] (WCU) has been used successfully in the analysis of light-scattering experiments.[2,5] The WCU equation specifically describes a molecular system with nondegenerate internal states. A more complicated kinetic equation, proposed later by Waldman[9] and Snider,[10] treats the effect of internal-state degeneracy. As pointed out by Sugawara and Yip,[2] however, the distinction between these two approaches is blurred by the fact that neither equation is mathematically tractable without approximation.

Sugawara and Yip[2] and Boley *et al.*[5] analyze light-scattering experiments in molecular gases on the basis of similar relaxation-time kinetic models that are based on the WCU kinetic equation. In the work of Sugawara and Yip, which we follow in the remainder of this paper, the solution for the spectral function $S(\vec{K}, \omega)$ depends generally on three parameters: the internal specific heat and the elastic and inelastic collision frequencies, σ_e and σ_i, respectively. The internal specific heat may be determined either from spectroscopic data[11] or from specific-heat measurements.[12] The presence of two collision frequencies, within the framework of this kinetic model, distinguishes polyatomic from monatomic gases. As pointed out by Sugawara and Yip,[2] in the limit of small σ_i their kinetic model reduces to that of Bhatnager, Gross, and Krook[13] for monatomic gases.

In this paper, we present the results of light-scattering experiments in the molecular gas N_2. The kinetic model of Sugawara and Yip is applied to the analysis of these experiments. A least-χ^2 procedure is used to obtain a best fit between theoretical and experimental spectral profiles as a function of the elastic and the inelastic relaxation times, both treated as adjustable parameters. The transition region between the collisionless and the kinetic descriptions of the gas dynamics is

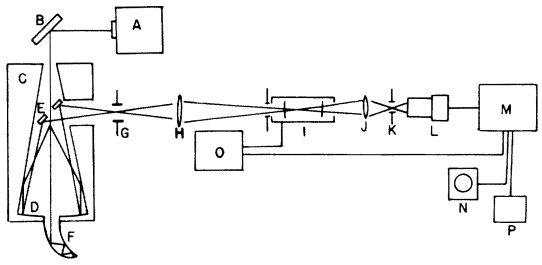

FIG. 1. Experimental light-scattering apparatus: A, laser; B, plane mirror; C, scattering cell; D, spherical mirror; E, circular plane mirror; F, Wood's cone; G, K, aperture stops; H, J, lenses; I, FPS interferometer; L, photomultiplier tube; M, 128-channel analyzer; N, oscilloscope; O, ramp generator; P, printer.

specifically probed in order to investigate the dependence of these parameters on collision frequency. A comparison between the least-χ^2 values of the relaxation times obtained from these measurements and from other experiments is given. Section II discusses the experimental procedure. The experimental results are presented in Sec. III. In Sec. IV, we analyze the results of these experiments from the point of view of the information they provide about rotational-relaxation phenomena in molecular gases.

II. EXPERIMENTAL CONSIDERATIONS

The spectral distribution of light scattered from density fluctuations in N_2 has been measured for pressures from 1 to 661 Torr at a temperature of 24.7 °C. Figure 1 illustrates the experimental arrangement. The beam from a single-mode frequency-stabilized He-Ne laser (wavelength 0.6328 μm) is directed along the axis of a conical scattering cell that is filled with spectrographic-grade N_2 gas; a Wood's cone absorbs the residual laser beam that is not scattered within the cell. Light scattered at the angle $\theta=15°$ from the forward direction is reflected by the conical surface parallel to the cell axis to the end spherical mirror whose focal point lies on the axis of the cell. This light is reflected from a circular, plane mirror and brought to a real focus in the plane of an aperture stop located just outside of the cell. Light transmitted by the aperture is imaged onto the central plane of a spherical mirror, piezoelectrically scanned Fabry-Perot interferometer (FPS) and subsequently detected by means of a cooled photomultiplier tube. The signal from the photomultiplier is processed by photon-counting electronics and displayed on a multichannel analyzer. The recorded spectrum is the convolution of the instrumental profile of the FPS with the scattered-light spectrum. Several features of the experimental apparatus merited special attention; these are discussed below.

Conical reflectors have the disadvantage that a portion of the light collected by the optical system may arise from multiple reflections within the cell. The primary signal that results from scattering at $\theta=2\alpha$ (where $\alpha=7.5°$ is the semiapex angle of the cone) and a subsequent single reflection at the conical surface may also contain light initially scattered at $\theta=4\alpha, 6\alpha, \ldots,$ and undergoing 2,3,..., reflections at the conical surface. Geometrical arguments show that these spurious, multiply reflected components arise from initial scattering of the laser beam from axial regions that are farther from the spherical mirror than is the region for singly reflected light. In the present experiment, these additional axial-scattering regions are effectively blocked from the collection optics by a judicious choice of the size, shape, and location of the circular, plane mirror. The collected light thus consists solely of light scattered at the angle $\theta=2\alpha$.

Each sweep of the spectrum is initiated by means of a trigger pulse from the multichannel analyzer to a ramp voltage generator which, in turn, sweeps the instrumental bandpass of the FPS (~40 MHz) across the spectrum of the scattered light at a uniform rate. The spectrum is swept a sufficient number of times, with a duration of 10 sec per sweep, in order to achieve adequate counting statistics. A nonrandom drift in the output frequency of the laser, ~0.1 MHz/min after a warm-up period of 24 h, limits the real time required to obtain a spectrum to be $\lesssim$15 min. This restriction is only operative for spectral runs at cell pressures ~ a few Torr; for higher pressures, real times less than 15 min are required to obtain adequate signal levels.

The background counting rate is determined by obtaining a spectral profile in the manner described in the preceding paragraph when the scattering cell is evacuated. This background signal, due primarily to spurious reflections of the incident laser beam within the cell, is measured for several spectral runs and an average background signal profile obtained. The spectral profiles described in the following section are each corrected for this average background profile. The background fluctuations are also incorporated into the total statistical fluctuations of the observed spectral signals.

III. EXPERIMENTAL RESULTS

The spectral profiles depend generally on the ratio of the characteristic wavelength λ_f to the mean free path. For monatomic gases, the spec-

tra may be classified in terms of an ordering parameter[14] $y=\sigma/Kv_0$, where σ is the collision frequency and v_0 the mean molecular speed. The regions $y \ll 1$ and $y \gg 1$ correspond to the collisionless and the hydrodynamic limits, respectively. In this paper, we will be concerned with $y \lesssim 1$, the transition region between the collisionless and the kinetic regime. For molecular gases, it is necessary to distinguish elastic from inelastic collisions. Sugawara and Yip incorporate this feature of light scattering in molecular gases by defining two collision frequencies, σ_i and σ_e, that describe inelastic and elastic collisions, respectively, where $\sigma=\sigma_i+\sigma_e$. Two ratios of fluctuation wavelength to mean free path are then significant in the description of the spectrum. The spectral profiles may still be ordered by means of the parameter y. A second parameter $\alpha=\sigma_i/\sigma_e$ is now required, however, to give a complete description of the kinetic model.

The quantities σ and α may be obtained[2] from thermodynamic measurements. We define a thermodynamic collision frequency $\sigma_T=P/\eta_s$ obtained in this way, where P is the pressure in the scattering cell and η_s is the shear viscosity. Thermal transpiration measurements,[15] among others, yield a value of the ratio α in terms of the rotational relaxation number Z_{rot}. We define a thermodynamic ratio obtained in this way by $\alpha_T=(Z_{\text{rot}}-1)^{-1}$. Alternatively, σ and α may be defined by a procedure which produces the best fit between experimental and theoretical spectral profiles. We define $\sigma_{\min}$ and $\alpha_{\min}$ to be the values of σ and α obtained by this latter method. In the experiments reported in this paper, certain discrepancies are observed between the thermodynamic and the spectral values of these constants. The nature of these discrepancies are discussed in the following paragraphs.

Figure 2 illustrates representative experimental spectral profiles (closed circles) obtained with the apparatus described in the preceding section. The profiles shown are for values of y_T $(=\sigma_T/Kv_0)$ $=4.39$, 1.05, 0.55, and 0.007 corresponding to cell pressures of 641, 154, 81 and 1 Torr, respectively. Also shown are theoretical profiles (solid curves) obtained by convolving the instrumental profile of the FPS with the solution to the kinetic model equation of Sugawara and Yip. Units along the abscissa are given in terms of a normalized frequency parameter $x=\omega/Kv_0$. A least-χ^2 fitting procedure[16] is used to obtain the theoretical profiles illustrated in Fig. 2. χ^2 is considered to be a continuous function of the parameters σ and α. The surface $\chi^2(\sigma, \alpha)$ is scanned in order to obtain the minimum value of χ^2, and hence determine $\sigma_{\min}$ and $\alpha_{\min}$. The error bars associated with the experimental points in Fig. 2 give the rms variation in the (signal + background) in the ith frequency channel of the analyzer.

The agreement between theory and experiment is seen from Fig. 2 to be generally good. Small deviations are to be noted in the saddles between the Rayleigh and Brillouin peaks, and at the Brillouin peaks, of the $y_T=4.39$ spectrum. This discrepancy is thought to be due to a failure of the convolution precedure to adequately account for the contribution of the instrumental linewidth to the observed spectral profile. The wing of the smallest $y=0.007$ profile shows a similar small discrepancy. Data points in the wing of this spectrum require long integration times. The laser drift discussed in the preceding section is believed to have introduced a nonrandom error into the data in this spectral region, thereby causing the observed discrepancy between theory and experiment.

The spectrum of Fig. 2(a) for $y_T=4.39$ exhibits the Rayleigh-Brillouin triplet structure that is characteristic of the hydrodynamic limit. Figure 2(a) does not represent a hydrodynamic spectrum, however. This may be seen from a comparison of the sound velocity, as computed from the Brillouin shift in Fig. 2(a), with the sound velocity as measured by conventional ultrasonic methods.[12] The former velocity may be computed to be 342 m/sec whereas the latter value is 351.5 m/sec. The measured sound velocity from Fig. 2(a) does not agree, within experimental uncertainty, with the hydrodynamic value. We interpret this discrepancy as being indicative of the importance of kinetic effects in the formation of the spectrum of Fig. 2(a).

Table I lists values of σ_T, $\sigma_{\min}$, and $\alpha_{\min}$ for a range of pressures from 1 to 661 Torr. The spectral profiles specifically illustrated in Fig. 2(a)–(d) are labeled in Table I with superscripts (a)–(d), respectively. A discrepancy between σ_T and $\sigma_{\min}$ is seen to exist for pressures of 524 Torr and higher that is outside the experimental uncertainty in either quantity. For pressures less than 524 Torr, experimental uncertainties are sufficiently large that the observed differences must be viewed with caution. In particular, note that $\sigma_{\min}=0$ provides the best fit for pressures <6 Torr. The values of $\alpha_{\min}$ are seen to rise abruptly as the pressure is reduced from 661 Torr. At a pressure where σ_T and $\sigma_{\min}$ come into agreement (within experimental uncertainty), $\alpha_{\min}$ reaches a constant value of 0.35. This constant value is maintained until a pressure of 136 Torr is reached. Below 136 Torr, the value of $\alpha_{\min}$ at first oscillates and subsequently drops to zero. Below 37 Torr, note that $\alpha_{\min}=0$ provides the best fit between the theory of Sugawara and Yip and the experimental spectral

profiles. The value $\alpha_{min} = 0.35$ agrees within experimental error with the theoretical expression obtained by Parker,[17] and is in near agreement with results of ultrasonic measurements obtained by a number of investigators.[18-21]

The behavior of the individual collision frequencies, σ_i and σ_e, may be easily determined from the measured values of σ_{min} and α_{min}. In Fig. 3, we have plotted the measured values of σ_i and σ_e vs σ_T. We see that σ_e is a monotonically increasing function of σ_T. The inelastic collision frequency σ_i, however, falls to 0 faster than σ_e at small values of σ_T and again decreases for the largest values of σ_T. The behavior of σ_i for small values σ_T is responsible for $\alpha_{min} = 0$, providing the best fit between theory and experiment at low gas pressures. The reduction in σ_i at the largest values of σ_T is responsible for the reduction of α_{min} at the largest gas pressures.

IV. SUMMARY AND DISCUSSION

In this paper, experimental spectral profiles of light scattered in molecular nitrogen have been compared with theoretical profiles calculated by means of the kinetic model equations of Sugawara and Yip. Two constants that appear in the kinetic model description of the molecular dynamics, the combined collision frequency σ and the ratio of inelastic to elastic collision frequencies α, are treated as adjustable parameters. A least-χ^2 fit between experimental and theoretical spectral profiles is obtained as a function of these two parameters.

The agreement with the theory of Sugawara and Yip is good. There are observed differences, however, between σ_{min} and α_{min}, values of the parameters σ and α that result in the least-χ^2 fit between experiment and theory, and values σ_T and

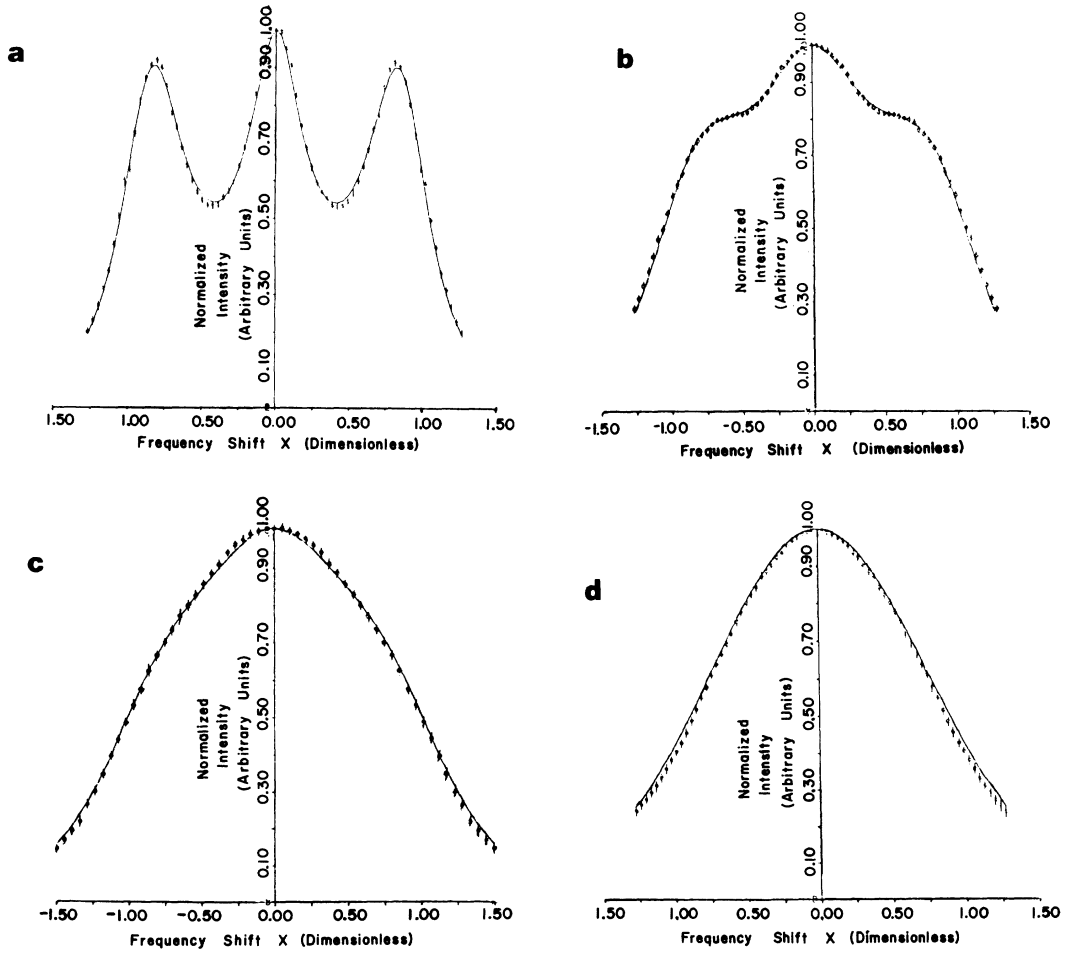

FIG. 2. Spectral profiles: (a) $P = 641$ Torr, $y_T = 4.39$, $\sigma_{min} = 4.39 \times 10^9$ Hz, $\alpha_{min} = 0.29$; (b) $P = 154$ Torr, $y_T = 1.05$, $\sigma_{min} = 1.25 \times 10^9$ Hz, $\alpha_{min} = 0.35$; (c) $P = 81$ Torr, $y_T = 0.55$, $\sigma_{min} = 0.55 \times 10^9$ Hz, $\alpha_{min} = 0.21$; (d) $P = 1$ Torr, $y_T = 0.007$, $\alpha_{min} \simeq 0$, $\sigma_{min} = \simeq 0$. Experimental points (closed circles with error bars). Theoretical spectrum is solid curve. $x = \omega/Kv_0$.

α_T determined from hydrodynamic measurements. In this experiment, a study is made of the transition region between the collisionless limit and the kinetic regime, corresponding to gas pressures from 1 to 661 Torr. At pressures larger than approximately 524 Torr, a discrepancy is observed between σ_{min} and σ_T that is outside the experimental uncertainty of either value. The gas pressure P is known to an accuracy $\lesssim \pm 1$ Torr. Assuming that the kinetic model of Sugawara and Yip provides an accurate description of the spectra in this pressure range and that the internal specific heat may be adequately determined from spectroscopic data, the difference between σ_{min} and $\sigma_T (= P/\eta_s)$ results from a departure of the shear viscosity η_s from the hydrodynamic value in this pressure regime. From Table I the relative difference $|\sigma_T - \sigma_{min}|/\sigma_{min}$ is seen to increase as the pressure is reduced. Experimental error in this lower-pressure regime is unfortunately also large. This experiment should be repeated with increased signal-to-noise ratio (e.g., by using a higher-power laser and/or longer integration times) to allow a more precise determination of this difference at lower pressure.

The value $\alpha_{min} = 0.35$ provides good agreement between theory and experiment over a range of gas pressure $136 \lesssim P \lesssim 524$ Torr. In this pressure range α_{min} agrees within experimental error with the theoretical value obtained by Parker[17] (we denote this quantity by α_T) and is reasonable agreement with the results of ultrasonic measurements.[18-21] In the pressure region $\gtrsim 524$ Torr, α_{min} deviates from α_T declining sharply in value. Sugawara and Yip[2] have also noted that a smaller value of α provides better agreement between theory and experiment at the larger values of y.

The ratio α_{min} exhibits a similar departure from α_T in the low-pressure region. The error bars in this region are large, and the following discussion is therefore only qualitative. The spectrum of light scattered at the angle θ is a probe of the temporal behavior of fluctuations in the gas that occur within a microscopic scattering volume with a scale length $\lambda_f = 2\pi/K$. The frequency scale of these measurements is[22] $\Delta\nu_s = \omega_s/2\pi \simeq Kv_0/2\pi$ as long as the instrumental width $\Delta\nu_{FPS}$ may be neglected. In this experiment, $\Delta\nu_{FPS} \cong 40$ MHz forms an absolute-minimum-frequency scale with which to probe the temporal behavior of density fluctuations. Two ordering parameters may be defined for the case of a molecular gas, $y_i = \sigma_i/\omega_s$ and $y_e = \sigma_e/\omega_s$. In the region $136 \lesssim P \lesssim 524$ Torr, $\sigma_i/\sigma_e = \alpha_{min} \cong 0.35$ and both σ_i and σ_e decrease with decreasing pressure. The inelastic collision frequency σ_i will then become comparable to the scale frequency at a pressure where σ_e is significantly larger than $\Delta\nu_s$. Below this value of the pressure, the inelastic collisions are increasingly frozen out and the spectral profile should approach that for a monatomic gas. At a still lower pressure, σ_i becomes comparable with $\Delta\nu_{FPS}$ and the spectral measurements are insensitive to the internal degrees of freedom of the molecules. The collisionless limit will be reached, in the spirit of this discussion, when both σ_i and σ_e become smaller than $\Delta\nu_{FPS}$. This argument may be given equivalently in terms of the relaxation times τ_i and τ_e. For example, the internal degrees of freedom begin to be frozen out when the pressure is reduced to the point where $v_0\tau_i$ becomes larger than the scale length λ_f.

The above discussion may be placed on a semiquantitative basis. From Table I we see that α_{min}

TABLE I. Kinetic model parameters. [Superscripts (a)–(d) refer to the corresponding spectral profiles in Fig. 2.]

P (Torr)	$10^9\sigma_T$	$10^9\sigma_{min}$	α_{min}
661	4.92 ± 0.01	4.33 ± 0.18	0.15 ± 0.02
641[(a)]	4.78 ± 0.01	4.39 ± 0.15	0.29 ± 0.02
524	3.91 ± 0.01	3.51 ± 0.15	0.35 ± 0.02
431	3.21 ± 0.01	3.11 ± 0.20	0.35 ± 0.02
300	2.23 ± 0.01	2.05 ± 0.20	0.35 ± 0.02
154[(b)]	1.14 ± 0.01	1.25 ± 0.15	0.35 ± 0.02
136	1.01 ± 0.01	1.15 ± 0.20	0.35 ± 0.02
122	0.909 ± 0.007	0.908 ± 0.19	0.31 ± 0.02
101	0.752 ± 0.007	0.826 ± 0.15	0.18 ± 0.02
81[(c)]	0.603 ± 0.007	0.550 ± 0.15	0.21 ± 0.03
53	0.395 ± 0.007	0.395 ± 0.15	0.33 ± 0.03
37	0.275 ± 0.007	0.175 ± 0.10	0.11 ± 0.03
22	0.164 ± 0.004	0.084 ± 0.15	~0.0 ± 0.03
14	0.104 ± 0.004	0.054 ± 0.15	~0.0 ± 0.03
6	0.045 ± 0.003	0.0092 ± 0.10	~0.0 ± 0.03
3	0.022 ± 0.003	~0.0 ± 0.10	~0.0 ± 0.03
1[(d)]	0.0075 ± 0.0010	~0.0 ± 0.10	~0.0 ± 0.03

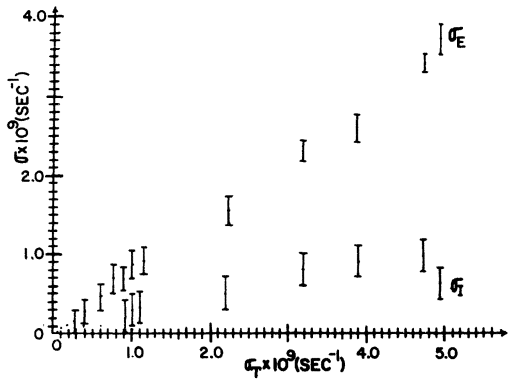

FIG. 3. Plot of σ_e and σ_i versus σ_T.

begins to deviate from α_T at a pressure ~122 Torr. At this pressure we find $\sigma_i \cong 210$ MHz which is comparable with the scale frequency for this experiment $\Delta\nu_s \cong 170$ MHz. For pressure $\lesssim 37$ Torr $\alpha_{\min} = 0$ provides the best fit between experiment and theory. For $P = 37$ Torr, $\sigma_i \cong 20$ MHz which is comparable to the instrumental bandwidth $\Delta\nu_{\mathrm{FPS}} \cong 40$ MHz. Finally, at a pressure $\lesssim 6$ Torr, σ_i and $\sigma_e = 0$ provides the best fit between theory and experiment. For $P = 6$ Torr, $\sigma_e \cong 10$ MHz is likewise comparable with the instrumental bandwidth. At this pressure, we have effectively reached the collisionless limit insofar as our light scattering measurements are concerned.

The experiments described in this paper could be profitably repeated with a longer scale length λ_f (achieved either by using a longer incident wavelength or a smaller scattering angle). This would permit observation of the dynamical behavior of these slower rotational relaxation processes.

---

*Present address: Sandia Laboratories, Albuquerque, N.M.

[1]T. J. Greytak and G. B. Benedek, Phys. Rev. Lett. 17, 179 (1966).
[2]A. Sugawara and S. Yip, Phys, Fluids 10, 1911 (1967).
[3]E. H. Hara, A. D. May, and H. F. Knaap, Can. J. Phys. 49, 420 (1971).
[4]A. Broz, M. Harrigan, R. Kasten, and A. Monkewicz, J. Acoust. Soc. Am. 49, 950 (1971).
[5]C. D. Boley, R. C. Desai, and G. Tenti, Can. J. Phys. 50, 2158 (1972); 52, 285 (1974).
[6]R. Pecora, J. Chem. Phys. 40, 1604 (1964).
[7]L. Van Hove, Phys. Rev. 95, 249 (1954).
[8]C. S. Wang Chang, G. E. Uhlenbeck, and J. deBoer, in *Studies In Statistical Mechanics*, edited by J. deBoer and G. E. Uhlenbeck (North-Holland, New York, 1964), Vol. II, Pt. C.
[9]L. Waldmann, Z. Naturforsch. 12a, 660 (1957); 13a, 609 (1958).
[10]R. F. Snider, J. Chem. Phys. 32, 1051 (1960).
[11]G. Herzberg, *Infrared and Raman Spectra of Polyatomic Molecules* (Van Nostrand, New York, 1945), Chap. V.
[12]*American Institute of Physics Handbook*, edited by D. E. Gray (McGraw-Hill, New York, 1963).
[13]P. F. Bhatnagar, E. Gross, and M. Krook, Phys. Rev. 94, 511 (1954).
[14]S. Yip and M. Nelkin, Phys. Rev. 135, A1241 (1964).
[15]A. P. Malinanskas, J. Chem. Phys. 44, 1196 (1966).
[16]P. R. Bevington, *Data Reduction and Error Analysis for the Physical Sciences* (McGraw-Hill, New York, 1969).
[17]J. G. Parker, Phys. Fluids 2, 449 (1959).
[18]A. J. Zmuda, J. Acoust. Soc. Am. 23, 472 (1951).
[19]J. G. Parker, C. E. Adams, R. M. Stravseth, J. Acoust. Soc. Am. 25, 263 (1953).
[20]W. Tempest and H. D. Parbrook, Acustica 7, 354 (1957).
[21]M. Greenspan, J. Acoust. Soc. Am. 30, 672 (1958).
[22]S. Yip, J. Acoust. Soc. Am. 49, 942 (1971).